Wear particle image segmentation using a two-stage strategy

Heng-guang Guo[1*], Jun Qu[2]

[1]*Graduate Students' Brigade, Naval Aeronautical Engineering Institute, Yantai, 26400, China*

[2]*Department of Airborne Vehicle Engineering, Naval Aeronautical Engineering Institute, Yantai, 264001, China*

Received 1 October 2014, www.cmnt.lv

Abstract

Wear particle image analysis is an effective and reliable method for equipment condition monitoring and fault diagnosis. Segmenting wear particle from image is an important but challenging problem. In this paper, a two-stage wear particle image segmentation strategy is presented, which consists of a rough segmentation stage and a fine segmentation stage. In the first stage, a wear particle image is divided into blocks, and clustering method is used to group blocks. This stage aims to get the rough boundary of the wear particle. In the second stage, color gradient is introduced into GVF snake to establish color GVF snake model, and rough boundary from the first stage is used as initial contour. This stage tries to extract the accurate boundary of the wear particle. Experimental results shows that the method proposed in this paper offers an accurate, minimally interactive, and efficient scheme for wear particle image segmentation, and increases the quality of wear particle image segmentation in compare with some state-of-art segmentation methods.

Keywords: wear particle image segmentation, two-stage strategy, snake model, color gradient, color GVF snake

1 Introduction

By analyzing the wear particles in the lubricant oil, wear condition, wear mode, and wear mechanism of mechanical equipment can be estimated, and according to these information, equipment condition monitoring and fault diagnosis can be achieved [1-3]. For the effective accomplishment of the task, wear particle image analysis offers the most promising prospects for success. By analyzing the wear particle image, wear particle features, such as shape feature, texture feature, and color feature, can be extracted. According to these features, wear particle type can be recognized, and wear faults can be diagnosed intelligently [4-8]. Wear particle image analysis contains three steps: image segmentation, feature extraction, and wear particle classification. Wear particle image segmentation is the first step, and is also a very important step. The results and accuracy of wear particle image segmentation can affect the feature extraction, classification and recognition of wear particle directly.

Image segmentation is the process of dividing the interested region of the image from its background, in order to delineate or extract features of the region. Snakes or active contour models [9], have gained significant attention and are widely used in many applications, including image segmentation [10, 13], edge detection [14, 15], shape modelling [16, 17]. In the process of image segmentation, snake is an energy-minimizing curve controlled by the internal force and the external force that pull it towards the object's boundary in the image. In order to solve the problems associated with initialization and poor convergence to boundary concavities, Xu and Prince developed a new external force, called gradient vector flow (GVF) [18, 19], which largely solves the problems.

In order to improve the accuracy of wear particle image segmentation, this paper proposed a two-stage strategy, which consists of a rough segmentation stage and a fine segmentation stage. In the rough segmentation stage, the wear particle image is divided into blocks, and the rough boundary of the wear particle can be got by using block clustering method based on color and texture features. In the fine segmentation stage, the wear particle rough boundary is used as the initial contour of the GVF snake model, and color gradient of the image is added into the model. At last, accurate of the wear particle can be extracted after iteration.

2 Wear particle image rough segmentation

The aim of wear particle image rough segmentation is to determine the rough boundary of the wear particle in the image, and use it as the initial contour of the GVF snake model. In the rough segmentation stage, first, the wear particle image is divided into non-overlapping blocks with $M \times M$ pixels, and there exists N blocks in the image. In order to make a compromise between effectiveness and computation time, the size of the block is 5×5. Second, color feature and texture feature are extracted for each block. At last, the *k-means* clustering method is applied to the set of blocks, and these blocks can be grouped into several clusters. After clustering, the rough boundary of wear particle image can be located.

2.1 COLOR FEATURE EXTRACTION

Color feature, the basic and direct feature of color image, has been widely used in color image segmentation. Color feature extraction is always executed in RGB color space,

[*] ***Corresponding author's*** e-mail: guohengguang@126.com

but the values of R, G, and B components have no direct relationship with the three basic visual characteristics (luminance, hue, saturation) [20]. In this paper, the color feature is calculated in the CIE *La*b** color space, which is more coincident with human visual characteristic.

The color feature includes three average values of the color component in a block, i.e., the L, *a**, *b** components in the CIE *La*b** color space. For each block $B_i (i = 1,2,...,N)$, the color feature vector C_i is defined as:

$$C_i = \left[\frac{1}{M \times M} \sum_{j=1}^{M \times M} p^i_{j\_L}, \frac{1}{M \times M} \sum_{j=1}^{M \times M} p^i_{j\_a^*}, \frac{1}{M \times M} \sum_{j=1}^{M \times M} p^i_{j\_b^*} \right]^T \quad (1)$$

where, $p^i_{j\_L}$, $p^i_{j\_a}$, and $p^i_{j\_b^*}$ denote the three color component value of the pixel p^i_j in block B_i.

2.2 TEXTURE FEATURE EXTRACTION

The delineation of texture depends on scale strongly, and in order to reduce the sensitivity to scale, the texture can be described using multi-scale methods. Wavelet transform is a very important texture feature extraction method that based on signal processing, and has been widely used in image texture feature extraction. In this paper, in order to extract the texture feature, a wavelet transform is applied to the *L* component. After a one-level transform, the image is decomposed into four frequency bands: LL, LH, HL, and HH. For each block B_i, its texture feature is defined as:

$$T_i = \frac{1}{M \times M} \left[\sum_{j=1}^{M \times M} c^i_{j\_LH}, \sum_{j=1}^{M \times M} c^i_{j\_HL}, \sum_{j=1}^{M \times M} c^i_{j\_HH} \right]^T, \quad (2)$$

where, $c^i_{j\_LH}$, $c^i_{j\_HL}$, and $c^i_{j\_HH}$ denote the band coefficients of pixel p^i_j in block B_i

a) Original wear particle image

b) Binary image after rough segmentation

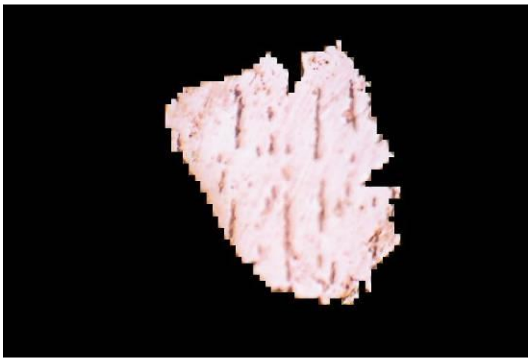

c) Wear particle image rough segmentation result

d) Rough contour of wear particle

FIGURE 1 Wear particle image rough segmentation

After the extraction of color feature and texture feature, each block of wear particle image has 6 features. Using k-means clustering method, the wear particle image rough segmentation can be achieved. In this paper, the goal of image segmentation is to divide the middle sever sliding wear particle in Figure 1a from its background. Figure 1b presents the binary image after rough segmentation. Figure 1c shows the result of wear particle image rough segmentation. Figure 1d presents the rough contour of wear particle acquired by wear particle image rough segmentation.

3 Color gradient

In grey level images, the gradient is defined as the first derivative of the image luminance. It has a high value in those regions exhibiting high luminance contrast. However, this strategy is not suitable for color images. Simply transforming color images into grey level images by taking the average of three channels and applying the grey level image gradient operator does not provide satisfactory results.

In this paper, color gradient adopts the definition in [21]-[23]. In contrast to previous approaches, the color gradient is defined in Luv color space rather than RGB color space, because Euclidean metric and distance are perceptually uniform in Luv color space, which is not the case in RGB color space.

For a color image Let $\Gamma(x,y):\Re^3$ be a color image, based on classical Riemannian geometry results. The L_2 norm can be written in matrix form

$$d\Gamma^2 = \begin{bmatrix} dx \\ dy \end{bmatrix}^T \begin{bmatrix} g_{11} & g_{12} \\ g_{21} & g_{22} \end{bmatrix} \begin{bmatrix} dx \\ dy \end{bmatrix}, \tag{3}$$

where

$$\begin{aligned} g_{11} &= \left[\frac{\partial \Gamma_1}{\partial x}\right]^2 + \left[\frac{\partial \Gamma_2}{\partial x}\right]^2 + \left[\frac{\partial \Gamma_3}{\partial x}\right]^2, \\ g_{12} = g_{21} &= \frac{\partial \Gamma_1}{\partial x}\cdot\frac{\partial \Gamma_1}{\partial y} + \frac{\partial \Gamma_2}{\partial x}\cdot\frac{\partial \Gamma_2}{\partial y} + \frac{\partial \Gamma_3}{\partial x}\cdot\frac{\partial \Gamma_3}{\partial y}, \\ g_{22} &= \left[\frac{\partial \Gamma_1}{\partial y}\right]^2 + \left[\frac{\partial \Gamma_2}{\partial y}\right]^2 + \left[\frac{\partial \Gamma_3}{\partial y}\right]^2. \end{aligned} \tag{4}$$

The matrix $\left[g_{i,j}\right] = \begin{bmatrix} g_{11} & g_{12} \\ g_{21} & g_{22} \end{bmatrix}$ contains the coefficients of the first fundamental form in the color space and is also referred to as the local structure tensor. It locally sums the gradient contributions from each image channel. Here Γ_1, Γ_2, and Γ_3 are intensities of each channel for any pixel in the image. The quadratic form Equation (3) achieves its extreme changing rates in the directions of the eigenvectors of matrix $\left[g_{i,j}\right]$, and the changing magnitude is decided by its eigenvalues λ_+ and λ_-. The eigenvalues can be expressed by

$$\lambda_\pm = \frac{g_{11} + g_{22} \pm \sqrt{\Delta}}{2}, \tag{5}$$

where

$$\Delta = (g_{11} - g_{22})^2 + 4g_{12}^2, \tag{6}$$

The color gradient at any pixel can be expressed as

$$\nabla C = \sqrt{\lambda_+ - \lambda_-}, \tag{7}$$

where

$$\begin{aligned} g_{11} &= \left[\frac{\partial L}{\partial x}\right]^2 + \left[\frac{\partial u}{\partial x}\right]^2 + \left[\frac{\partial v}{\partial x}\right]^2, \\ g_{12} &= \frac{\partial L}{\partial x}\cdot\frac{\partial L}{\partial y} + \frac{\partial u}{\partial x}\cdot\frac{\partial u}{\partial y} + \frac{\partial v}{\partial x}\cdot\frac{\partial v}{\partial y}, \\ g_{22} &= \left[\frac{\partial L}{\partial y}\right]^2 + \left[\frac{\partial u}{\partial y}\right]^2 + \left[\frac{\partial v}{\partial y}\right]^2. \end{aligned} \tag{8}$$

where *L*, *u*, and *v* are the three image channels of Luv color space.

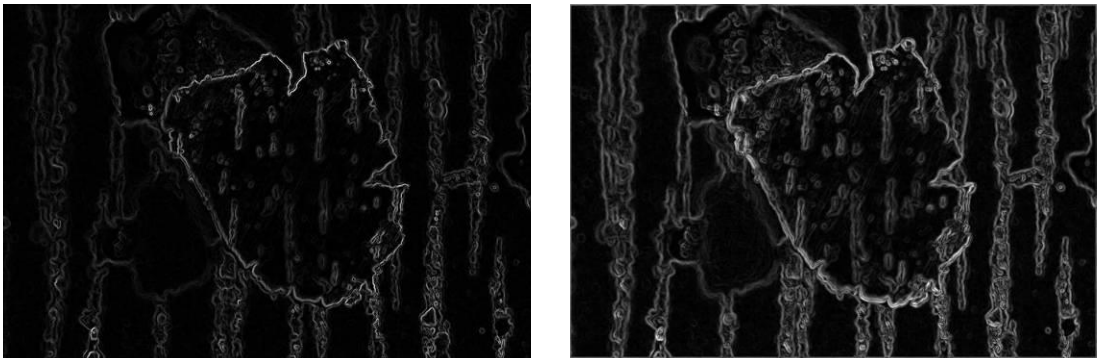

a) Grey gradient b) Color gradient

FIGURE 2 Wear particle image gradient

Figure 2 illustrates the role and importance of the color gradient function in driving the curve evolution for a snake model. The color gradient representation (Figure 2b) for the wear particle image (Figure 1a) results in more prominent boundary compared to the corresponding grey gradient (Figure 2a).

4 Wear particle image fine segmentation

4.1 SNAKE MODEL

Snakes, or active contours, are curves defined within an image domain that can move under the influence of internal forces coming from within the curve itself and external forces computed from the image data. There are two general types of active contour models: parametric active contours and geometric active contours. In this paper, parametric active contour is used. A traditional snake is a curve $\mathbf{x}(s) = [x(s), y(s)]$, $s \in [0,1]$, and it moves through the spatial domain of an image to minimize the energy. The energy function can be defined as:

$$E_{\text{snake}} = \int_0^1 (E_{\text{int}}(\mathbf{x}(s)) + E_{\text{ext}}(\mathbf{x}(s)))ds, \tag{9}$$

where, E_{int} denotes the internal energy, and E_{ext} denotes the external energy.

The internal force E_{int} is used to maintain the continuity and smoothness of the active contour during its deformation process. It can be defined as:

$$E_{\text{int}} = \frac{\left(\alpha |\mathbf{x}'(s)|^2 + \beta |\mathbf{x}''(s)|^2\right)}{2}, \tag{10}$$

where, α and β are weighting parameters that control the snake's tension and rigidity respectively. $\mathbf{x}'(s)$ and $\mathbf{x}''(s)$ are the first and second derivatives of $\mathbf{x}(s)$ with respect to s.

The external force E_{ext} is derived from the image so that it takes on its smaller values at the features of interest, such as boundaries. It is often defined as:

$$E_{\text{ext}} = -\left|\nabla\left\{G_{\sigma(x,y)} \cdot I(x,y)\right\}\right|, \tag{11}$$

where, I is the original image, $G_{\sigma(x,y)}$ is the two-dimensional (2-D) Gaussian kernel with σ as its standard deviation, and ∇ is a gradient operator.

The goal of the computation is to find the local minima of E_{snake}, defined in Equation (9). Based on Euler-Lagrange principle, Equation (9) has a minimum when

$$\alpha \mathbf{x}(s)'' - \beta \mathbf{x}(s)'''' - \nabla E_{\text{ext}}(v(s)) = 0, \tag{12}$$

where, $\mathbf{x}(s)''$ and $\mathbf{x}(s)''''$ denote the first and second derivatives of $\mathbf{x}(s)$ with respect to s, respectively.

In order to solve the Equation (12), the snake is made dynamic by defining $\mathbf{x}$ as the function of time t and s. Then, the partial derivative of $\mathbf{x}$ with respect to t is then set equal to the left hand side of Equation (12) as follows:

$$\mathbf{x}_t(s,t) = \alpha \mathbf{x}(s,t)'' - \beta \mathbf{x}(s,t)'''' - \nabla E_{\text{ext}}(\mathbf{x}(s,t)), \tag{13}$$

The solution to Equation (13) can be achieved by solving the discrete equations iteratively.

4.2 GRADIENT VECTOR FLOW

The traditional snake model has two difficulties. First, the initial contour must be close to the true boundary. Second, active contours have difficulty processing into boundary concavities [18, 19]. In order to solve these problems, Xu and Prince proposed a new external force, which called gradient vector flow. The gradient vector flow is defined as a vector field $\mathbf{v}(x,y) = [u(x,y), v(x,y)]$ that minimizes the energy function:

$$\varepsilon = \iint \mu(\nabla^2 \mathbf{v}) + |\nabla f|^2 |\mathbf{v} - \nabla f|^2 \, dxdy, \tag{14}$$

where, $\nabla^2 = \partial^2/\partial x^2 + \partial^2/\partial y^2$ is the Laplacian operator, and is applied to each spatial component of $\mathbf{v}$ separately. f is an edge map derived from the original image I. This edge map can be either gray level or binary valued. It is computed using $\left|\nabla\left\{G_{\sigma(x,y)} * I(x,y)\right\}\right|$. $\left|\nabla\left\{G_{\sigma(x,y)} * I(x,y)\right\}\right|$ is the gradient of the image I after Gaussian smoothing, with variance σ and mean 0. When $|\nabla f|$ is small, the energy is dominated by $\nabla^2 \mathbf{v}$, yielding a slowly varying field. On the other hand, when $|\nabla f|$ is large, the second term dominates the integrand, and is minimized when $\mathbf{v} = |\nabla f|$. The parameter μ is a regularization parameter governing the trade off between the first term and the second term in the integrand.

4.3 COLOR GVF SNAKE

Using Equation (13) as a starting point to define the color GVF snake, the external force ∇E_{ext} in Equation (13) is replaced with a color GVF field $\mathbf{v}$ in Luv color space, yielding

$$\mathbf{x}_t(s,t) = \alpha \mathbf{x}(s,t)'' - \beta \mathbf{x}(s,t)'''' + \mathbf{v}, \tag{15}$$

In color GVF snake, ∇ in Equation (14) is the Luv color gradient defined in Equation (7). The initial snake contour is obtained from wear particle image rough segmentation stage. By applying calculation of variation, it can be shown that minimizing the integral in Equation (14) is equal to solving the following equations:

$$\mu \nabla^2 u - (u - f_x)(f_x^2 + f_y^2) = 0, \tag{16}$$

$$\mu \nabla^2 v - (v - f_y)(f_x^2 + f_y^2) = 0, \tag{17}$$

Equation (16) and Equation (17) can be solved by treating u and v as functions of time and solving

$$u_t(x,y,t) = \mu\nabla^2 u(x,y,t) - [u(x,y,t) - f_x(x,y)]\cdot [(f_x(x,y)^2 + f_y(x,y)^2)], \quad (18)$$

$$v_t(x,y,t) = \mu\nabla^2 v(x,y,t) - [v(x,y,t) - f_x(x,y)]\cdot [(f_x(x,y)^2 + f_y(x,y)^2)]. \quad (19)$$

In order to set up an iterative solution, let the indexes *i*, *j*, and *n* corresponding to *x*, *y*, and *t*, respectively. And let the spacing between pixels be Δx, Δy, and the time step for each iteration be Δt.

The steps associated with wear particle fine segmentation stage are as follows:

1) The original image is transformed from RGB color space to Luv color space.

2) The edge map is computed of the transformed image according to the color gradient and Gaussian smoothing.

3) The rough boundary obtained from the rough segmentation stage, is used as the initial contour to start the color GVF snake. Because the initial contour is close to the accurate boundary, it can converge quickly and provide clear, inherently connected, and smooth contour.

5 Experiment results

In this section, the experimental results are presented for demonstrating the performance of the proposed method in this paper, and comparing the performance of several state-of-art image segmentation algorithms with the proposed method in this paper.

a) Initial boundary

b) Boundary after 5 iterations

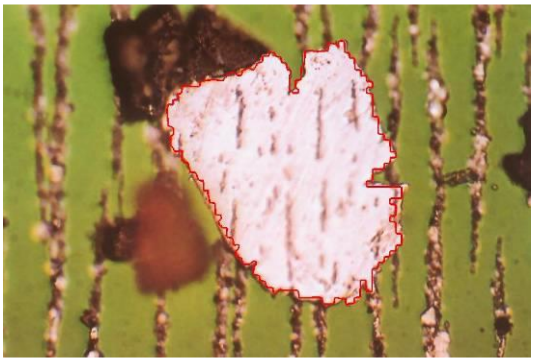

c) Boundary after 10 iterations

d) Final boundary

FIGURE 3 Wear particle image segmentation using color GVF snake

Figure 3 shows wear particle image segmentation using color GVF snake to segment the wear particle image Figure 1a. The red boundary in Figure 3a is the result of wear particle image rough segmentation, and it is used as the initial contour for color GVF snake model. Figure 3b shows the iterative result after 5 iterations, and Figure 3c shows the iterative result after 10 iterations. The last image Figure 3d is the iterative result after 25 iterations, and it is the final boundary. It can be seen from Figure 3 that even for the wear particle image have complex background, a complete separation of wear particle and the background within a picture can be fulfilled by the proposed two-stage strategy.

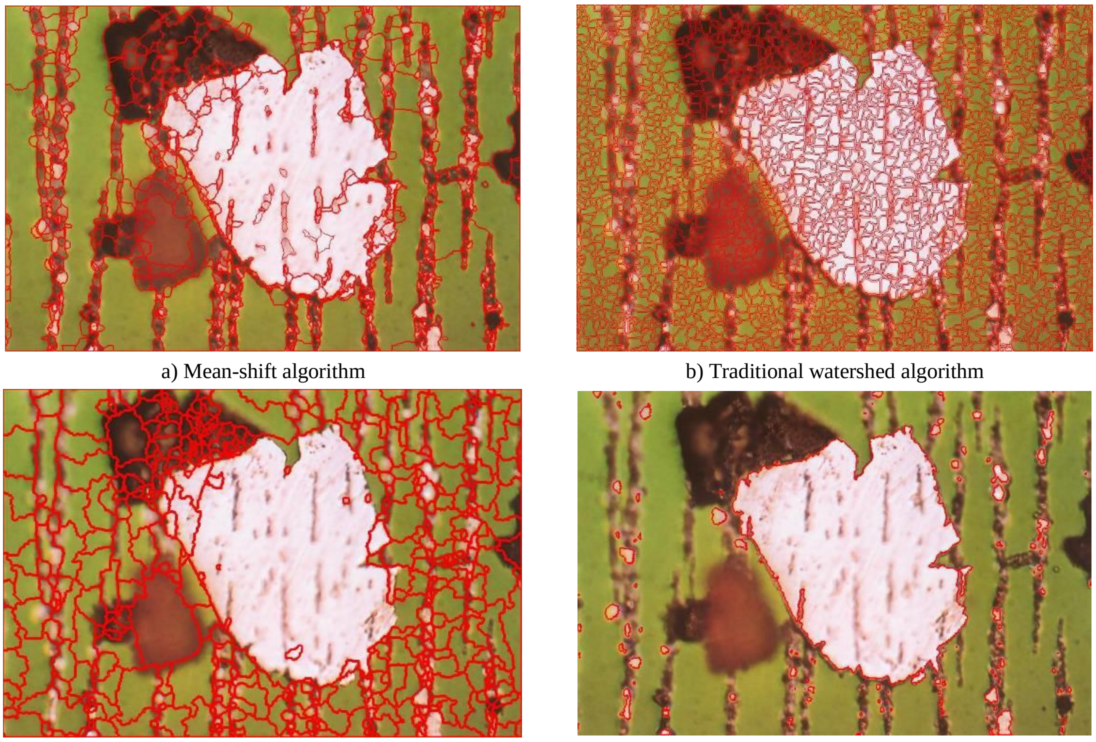

a) Mean-shift algorithm b) Traditional watershed algorithm

c) Marked-based watershed algorithm d) Threshold algorithm

FIGURE 4 Wear particle image segmentation comparison

In Figure 4, the performance of several state-of-art image segmentation algorithms is shown. Figure 4a shows the segmentation result of mean-shift algorithm [24]. The segmentation result using the traditional watershed algorithm is shown in Figure 4b. Figure 4c shows the segmentation result of marked-based watershed algorithm [25]. The segmentation result using the threshold algorithm is shown in Figure 4d. The result shows that the mean-shift segment the wear particle accurately, including even the holes within the wear particle region, and that means the wear particle has been oversegmented. However, to achieve accurate result, human intervention is required for manually merging the oversegmented regions. The watershed algorithm oversegments the wear particle image into a myriad of small regions, and that is impractical for application. Marked-based watershed algorithm was proposed to resolve oversegmentation problems. In wear particle image segmentation, it reduces the number of oversegmented regions significantly compared with traditional watershed algorithm, but still requires region merging to achieve useful result. The threshold algorithm gets the best segmentation result in comparison with the three other algorithms, but it still have oversegmentation problem. In the experiments, the two-stage method proposed in this paper provides the most accurate segmentation result, and maintains smooth boundary.

6 Conclusion

Wear particle image segmentation is an important stage in wear particle analysis based on image analysis. This paper has presented a two-stage strategy for wear particle image segmentation, which includes rough segmentation stage and fine segmentation stage. In the rough segmentation stage, the wear particle image is divided into blocks, clustering method is used to segment the image based on color and texture features of blocks, and the rough boundary is got at the end. In the fine segmentation stage, the rough boundary is treated as the initial contour, color gradient is introduced into the GVF snake model, and color GVF snake model is established and used to get the accurate wear particle boundary after iteration. Experimental results shows that the method proposed in this paper offers an accurate, minimally interactive, and efficient scheme for wear particle image segmentation. Following issues will be considered in the future research. First, more image attributes will be incorporate as features, and be added into the existing joint feature vector. Second, the applicability of the proposed method will be further extended, and be made more robust and practical.

Acknowledgments

The author is extremely grateful to Professor Qu Jun, and Professor Hu Guocai from the Department of Airborne Vehicle Engineering of Naval Aeronautical Engineering Institute. Thanks for all of their support and direction, as well as for selecting representative case.

References

[1] Kirk T B, Panzera D, Anamalay RV and Xu Z L 1995 Computer image analysis of wear debris for machine condition monitoring and fault diagnosis *Wear* (184) 717-22

[2] Peng Z, Goodwin S 2001 Wear-debris analysis in expert systems *Tribology Letters* **11** 177-84

[3] Surapol R 2005 Wear particle analysis - utilization of quantitative computer image analysis: A review *Tribology International* **38**, 871-78

[4] Wahlstrom J, Olander L, Olofsson U 2010 Size, shape, and elemental composition of airborne wear particle from Disc brake materials *Tribology Letters* **38** 15-24

[5] Laghari M S 2003 Recognition of texture types of wear particles *Neural Compute & Applic* **12** 18-25

[6] Stachowiak G P, Podisiadlo P, Stachowiak G W 2006 Shape and texture features in the automated classification of adhesive and abrasive wear particles *Tribology Letters* **24** (1) 15-26

[7] Stachowiak G P, Stachowiak G W, Podsiadlo P 2008 Automated classification of wear particles based on their surface texture and shape features *Tribology International* **41**, 34-43

[8] Stachowiak G P, Podisiadlo P, Stachowiak G W 2005 A comparison of texture feature extraction methods for machine condition monitoring and failure analysis *Tribology Letters* **20**(2) 133-47

[9] Kass M, Witkin A, Terzopoulos D 1988 Snakes: active contour model *International Journal of Computer Vision*, (4) 321-31

[10] Qi Ge, Liang X, Zhi H W 2013 Active contour model for simultaneous MR image segmentation and denoising *Digital Signal Processing* **23** 1186-96

[11] Chen Q, Sun Q-s, Xia D-s 2013 Serial slice image segmentation of digital human based on adaptive geometric active contour tracking *Computer in Biology and Medicine* **43** 635-48

[12] Wang W, Zhu L, Qin J, Chui Y-P, Li B N, Heng P-A 2014 Multiscale geodesic active contours for ultrasound image segmentation using speckle reducing anisotropic diffusion *Optics and Lasers in Engineering* **54** 105-16

[13] Wang H, Huang T-Z, Zu Z, Wang Y 2014 An active contour model and its algorithms with local and global Gaussian distribution fitting energies *Information Sciences* **263** 43-59

[14] Gao J, Lei Z, Wang Z, Yan K 2011 Canny-based active contour accurate locating *Energy Procedia* **13** 4562-66

[15] Wang K, Guo Li 2012 Research of active contour model in aerial images *Physic procedia* **33** 542-47

[16] Qi Li, Chandra K 2011 Contour extraction of drosophila embryos *IEEE Transactions on Computer Biology and Bioinformatics* **8**(6) 1509-21

[17] John C, Xianghua Xie, Majid M 2012 Automatic bootstrapping and tracking of object contours *IEEE Transactions on Image Processing* **21**(3) 1231-45

[18] Chenyang Xu, Jerry L P 1998 Generalized gradient vector flow external forces for active contour *Signal Processing* **71** 131-39

[19] Chenyang Xu, Jerry L P 1998 Snakes, shapes, and gradient vector flow *IEEE Transactions on image processing* **7**(3) 359-69

[20] Wang X-Y, Wang Q-Y, Yang H-Y 2011 Color image segmentation using automatic pixel classification with support vector machine *Neurocomputing* **74** 3898-911

[21] Zenzo S D 1986 A note on the gradient of a multi-image *Computer Vision Graphics, and Image processing* **33** 116-25

[22] Sapiro G, Ringach D L 1996 Anisotropic diffusion on multivalued images with application to color filtering *IEEE Transactions on Image Processing* **5**(11) 1582-86

[23] Gevers T 2002 Adaptive image segmentation by combining photometric invariant region and edge information *IEEE Transaction on Pattern Analysis and Machine Intelligence* **24**(6) 848-52

[24] Comaniciu D, Meer P 2002 Mean shift: a roust approach toward feature space analysis *IEEE Transaction on Pattern Analysis and Machine Intelligence* **24** 603-19

[25] Moga A N 1998 Parallel marked-based image segmentation with watershed transformation *Journal of Parallel and Distribute Computing* **51** 27-45

Authors

Heng-guang Guo, November 8, 1986, Shandong, China.

Current position, grades: DS degree candidate.
University studies: BSc and MSc degrees in Naval Aeronautical Engineering Institute, Yantai, China, in 2008 and 2010, respectively.
Scientific interest: theory and diagnosis of mechanical system and image processing.
Publications: 3papers.

Jun Qu, September 4, 1962, Sichuan, China.

Current position, grades: professor with Department of Airborne Vehicle Engineering at the Naval Aeronautical Engineering Institute.
University studies: BS and MS degrees in Naval Aeronautical Engineering Institute Yantai, China.
Scientific interest: oil analysis, fuel analysis, NIR analysis technology, FTIR analysis technology.
Publications: 30 papers.